NANOSENSORS ENGINEERING: I. STRUCTURALLY MODULATED SnO_2 NANOWIRES

S. Dmitriev
Physics Department, Moldova State University,
60, A. Mateevici str., Chisinau, MD-2009, MOLDOVA

E-mail: sdmitriev@usm.md

Abstract – The results of research aimed at the gas sensing nanowires (NWs) engineering are presented. Structurally modulated SnO_2 NWs were obtained at 900^oC in the modified vapor-solid process, allowing that NW morphology could be encoded in a programmable way along its length. PVD technique was used for Ti/Au electrical contacts deposition and gas sensitive nanoscale chemiresistors formation.

Created nanostructures were characterized for their gas sensing performance. It was established that structurally-modulated NWs possess better gas sensitive characteristics in comparison with the straight ones. Obtained results are discussed from the positions of single-crystal "necks" formation in NWs.

Index terms: Nanostructure, Tin dioxide, Nanowire, Chemoresistor, Structural modulation, Morphology

1. INTRODUCTION

Recent publications [1-10] have demonstrated that metal oxide based one-dimensional nanostructures (NS) possess a huge potential for their application in the quality of chemical/gas and/or biosensors. This is connected with their generic chemical and thermal stability, their innate ability to transduce surface events into electrical signals and with two very important features of 1D nanostructures: 1) very high surface-to-bulk (*S/B*) ratio; 2) comparability of the Debye screening length L_D with the effective radius R of the conducting channel in NW. Both

these factors play determining role in the sensing performance of NS. In particular, the larger the *S/B* and L_D/R ratios of the active gas sensitive element the higher its sensitivity.

The performance of chemoresistor gas sensors (GS) and especially its sensitivity strongly depend on their materials-specific surface chemistry as well as the size and shape of their active elements. Nowadays, three basic approaches are used in the design of nanomaterials for GS. The first one is based on the fabrication of the very fine nanoparticles agglomerates in bulk or ultrathin film forms [11]; the second approach is connected with preparation of the metaloxide polycrystalline nanodimensional and nanostructured films [12-14]; and the third one relies on single crystal nanostructures (nanowire, nanorods, nanoribbons etc.) as sensing elements [1-6]. Both, high *S/B* and L_D/D ratios can be achieved using all three mentioned approaches. However, the first two approaches face the traditional challenges resultant from the unstable nature of the inter-granular interface, which determines the connectivity between grains [15] and hence the reliability, reproducibility and "lifetime" of the performance of the device. Thermo-mechanical and thermo-chemical instabilities of contacts are potentially another shortcomings of particle-aggregate-based gas sensors operating (as is often the case) at elevated temperatures and reactive environment.

The major advantage of single crystal quasi-1D sensors over traditional granular materials based sensors is their structurally and compositionally well-defined conducting channel which does not rely on inter-grain junctions for conductance. Thus, sensors based on single crystal metaloxide 1D nanostructures allow, in principle, to drastically improving of the majority of the aforementioned limitations. However, that to be able to meet competition with the best available polycrystalline film sensors operation parameters the nanowires, as sensitive elements of GS, should possess an effective diameter in the order of 10-20 nm. But such NS still belong to the size range where it is still challenging to produce nanostructures in a controllable way that to fabricate reliable electronic devices.

To overcome these technical challenges and to use in full degree the advantages of NW's crystallinity the next approach was developed based on utilization of the quasi-1D metal oxide nanostructures with modulated morphology as gas sensitive elements (GSE). Each such GSE may consists of a series of few micron long mesoscopic (200-300 nm in diameter) segments connected via ultra short and thin (tens of nanometers in length and diameter) ones. The physics behind this approach is illustrated schematically in Figure 1. For simplicity, only one section of

developed NW, consisting of two long and one short segment between them, is presented in Figure 1 for the idea illustration.

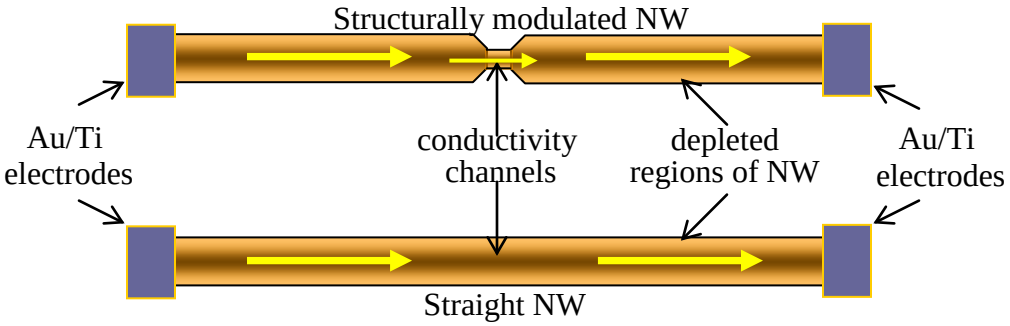

Figure 1. Structures of and electrical current in structurally modulated and straight metal oxide NW based GSE.

Here we have the NS with periodically alternating cross-section. It is important to note that in the contrast to granular structures, where the "necks" are formed by the contacts of neighboring grains and electrical current is modulated by Schottky barriers, in our case the "neck" region is part of the same single crystal NW and the electrical transport through such NS will be determined by the adsorbate-induced alternation in the effective cross-section of the conductivity channel. For comparison of the characters of electrical current passing the straight NW based GSE is also shown. Taking into account that physical/geometrical diameter of "neck" region of NW is, at least, of one order less than the diameter of basic part of NW we can expect that the sensitivity of this narrowed region to adsorption-desorption processes will be higher.

Thus, given experimental work was aimed to verify the proposed approach applicability to the gas sensing performance improvement of the structure modulated nanostructure based GSE.

II. EXPERIMENTAL DETAILS

Tin dioxide single-crystal structurally-modulated and also straight NWs were obtained via traditional vapor-solid process [16] in a Lindberg/Blue Scientific tube furnace at the temperature T=900°C from the powder precursor of research purity. However, there were used some modifications to the process on the basis of recently developed methodology [17] allowing to programming the morphology of metal oxide nanostructures during their synthesis. In brief, argon (99.998%), used as a carrier gas, was fed into a quartz tube through a solenoid valve activated by a computer-controlled power supply, allowing the argon gas flow to be shut off and

turned on in a programmable sequence. Varying the carrier gas flux during NW formation, we are capable not only to change the direction of NW growth and provide the changing of NW geometrical size but also we can technologically get the "necks" within the same single crystal.

X-ray diffraction (XRD) and Scanning Electron Microscopy were used to characterize the structure, composition and shape of the SnO_2 NWs.

Resist-free, Ti/Au (20/500 nm) PVD vacuum deposition through a shadow mask was used to produce Ohmic electrical contacts to individual segmented NWs to format the gas sensitive nanostructures.

The electrical (I-V) and gas sensing properties of the SnO_2 NWs were measured in the range -5 to +5 Volts in the two probe mode at the different temperatures (100-350°C) under vacuum ($P=5x10^{-6}$ Torr) and with sequential oxygen and hydrogen exposures in the range from $1x10^{-5}$ to $6x10^{-4}$ Torr. Gas pressure in the chamber was controlled by means of the pneumatic needle valves programmed by the *LabView* computer program.

III. RESULTS AND DISCUSSION

a) Structural characterization of SnO_2 nanowires

Figure 2 demonstrates XRD spectra of as-grown SnO_2 nanowires (both straight and structure modified) obtained in the 25-60º 2θ range. One can see that reflection peaks are very narrow that confirms that grown NWs are being highly crystalline. Observable peaks are characteristic for

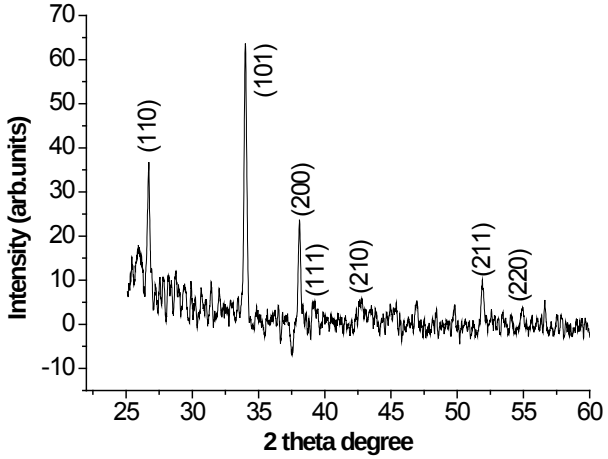

Figure 2. XRD spectrum of SnO_2 NWs

tetragonal (rutile) SnO_2 with domination of signal reflected from (101) crystallographic plane. Other peaks, obtained from (110) and (200) planes, are twice less by magnitude. As to the peaks assigned to (111), (210), (211) and (220) planes they are not very pronounced.

SEM image of the tin dioxide single-crystal structurally modified NW (SMNW), confined between two Au/Ti electrodes (Figure 3) shows that it consists of replacing each other well-faceted segments of different diameter. From TEM images (not presented here) it was estimated that effective diameters of changing segments are in the range from ~ 40 to about 280 nm. Lengths of both NWs have amounted 12-15 μm.

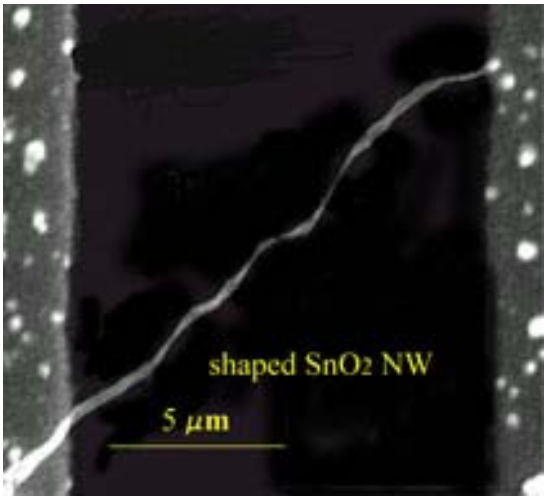

Figure 3. SEM image of SnO_2 SMNW with two Au/Ti electrodes.

b) Electrical and gas sensing characterization of SnO_2 nanowires

I-V curves of the tin dioxide SMNW were measured in the temperature interval from 100 to 350^{o}C (basic working diapason of gas sensors) in vacuum and in the presence of oxygen (P_{O2}=1x10^{-4} Torr) as oxygen plays exclusively important role in the gas detection processes, determining, in general, sensing performance of device. It was found that measured I-V curves are linear with applied voltage throughout the entire temperature range, implying ohmic contacts both under vacuum and in the presence of oxygen - an important factor if these nanostructures are to be exploited as sensors. Figure 4 shows one representative I-V dependence graph for T_{meas}=250^{o}C. However, one can see that in some degree the asymmetric behavior of curves is

observed. In particular, current magnitudes at ± 5 Volts are a little bit different for both vacuum and oxygen cases. It may be connected with a quite a bit different resistances between nanowires

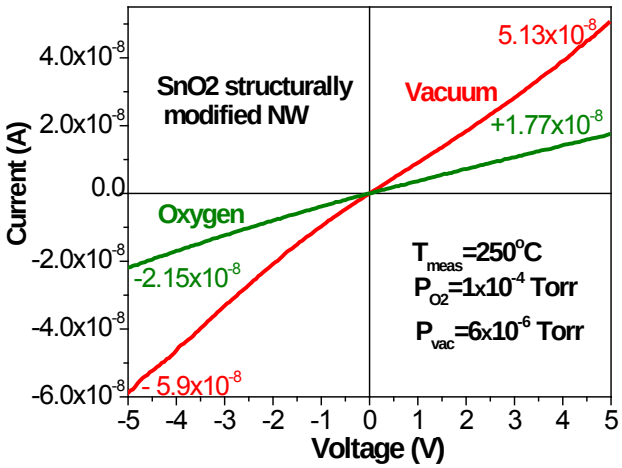

Figure 4. Typical I-V dependences of tin dioxide SMNW in vacuum and in the presence of O_2.

and electrodes themselves, i.e. different lengths of nanowire ends are covered with electrodes and as result different contact areas between NW and electrode for each NW's end.

It is interesting to estimate the ratio of the currents through NW in the presence of O_2 and under vacuum conditions, i.e. sensitivity to oxygen itself. In our case, the magnitude of ratio I_{oxy}/I_{vac} to $1x10^{-4}$ Torr oxygen is ca 2.8 that can provide the equivalent of sensitivity toward 100 ppb of O_2 dissolved in the inert gas being at atmospheric pressure. One can see that tin dioxide NWs are very sensitive to oxygen and can actively adsorb it. And also we observe the linear growth of $S_{oxy}= I_{oxy}/I_{vac}$ on dependence on applied voltage. However, large biases can lead to the NW destroying due to electrical breakdown so we restricted ourselves with ± 5 Volts range.

Figure 5 shows the calculated electron concentration *(n)* dependence on temperature derived from the obtained I-V data in oxygen presence. First of all, we should note that estimated from I-V data values of *n* are reasonable, i.e. are being in the characteristic for SnO_2 materials range 10^{18}-10^{20} cm^{-3}. Secondly, when plotted as *n*=f(T) two linear regions (100-200°C and 250-350°C) and a transition region (200-250°C) are observed for this function, which can be assigned to the peculiarities of the adsorption/desorption processes occurring at the SnO_2 nanowire surface. Namely, as it was shown for SnO_2 films, below 180°C the oxygen is adsorbed as a molecular species O_2^- [12]. From this temperature and up to ~250 °C the molecular oxygen undergoes the surface dissociation reaction $O_2 + e^- \rightarrow 2O^-$. The latter, in ideal case, should lead to the doubling

of the reactive oxygen species adsorbed on the surface and, as result, twofold decrease of the free carrier's concentration in the NW. In reality, the situation is quite different as one can see from

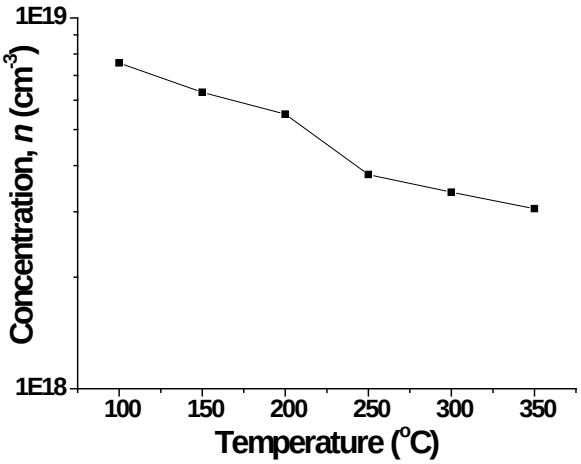

Figure 5. Dependence n=f(T) for tin dioxide SMNW in the O_2 presence.

Figure 5. In particular, the ratio n_{150}/n_{300} of the free electron concentrations at the 150 and 300°C correspondingly (taken from two linear regions) is equal to 1.93. This distinction from 2 can be stipulated by very different factors. In particular, as the reasons for observed discrepancy the next factors may be considered: 1) probability of the adsorption O^- radicals depends on the amount of the free surface sites available for adsorption; 2) inertion of adsorption–desorption processes; 3) state of the surface (cleanness). Nevertheless, we can state that features characteristic for thin film sensors are maintaining and at the nanometer level. The conductance activation energy, determined from log n=f(T) dependence, was in the range~ 80-100 meV corresponding to the energy range of the oxygen vacancy donor levels below the conduction band edge in SnO_2 [18].

Figure 6 demonstrates the typical SMNW response toward $3x10^{-4}$ Torr hydrogen pulses at the measurement temperature T=300°C. The magnitude of oxygen background was kept on the level $P_{O2}=1x10^{-4}$ Torr to provide required sensibilization level for SMNW. Baseline (see Figure 6) corresponds to the current through NW in the presence of background oxygen. One can see that H_2 leaking-in into the test chamber leads to the increase of conductivity through SMNW that corresponds to behavior of *n*-type material in the reducing atmosphere. Interaction of the hydrogen with chemisorbed oxygen is accompanied with electron release into the conduction band of SnO_2 nanowire and, as result, conductance growth.

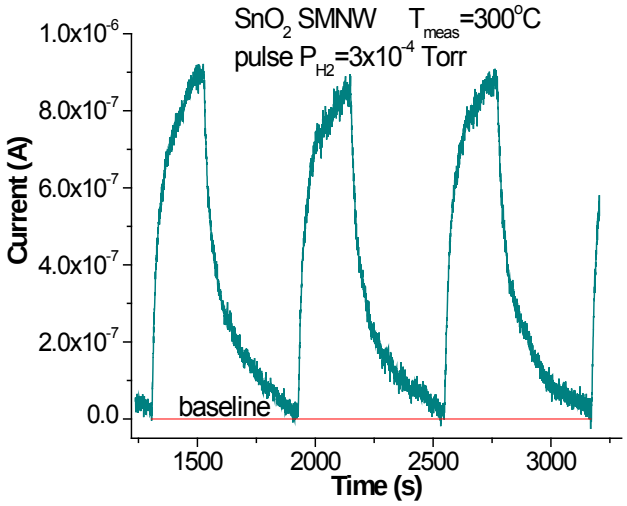

Figure 6. Current response of SnO_2 SMNW to hydrogen gas pulses

Results of the measurements of SMNW gas sensitivity toward H_2 (determined as $S=\Delta I/I_0 \cdot 100\%$) as a function of the operation temperature are presented in Figure 7. One can see that the temperature maximum of sensitivity toward hydrogen takes place at the temperature $T_{max}=200^{\circ}C$ and amounts 54%. Recalculation of hydrogen partial pressure from Torr to ppm gives the hydrogen concentration on the level 0.39 ppm (oxygen background - 0.13 ppm).

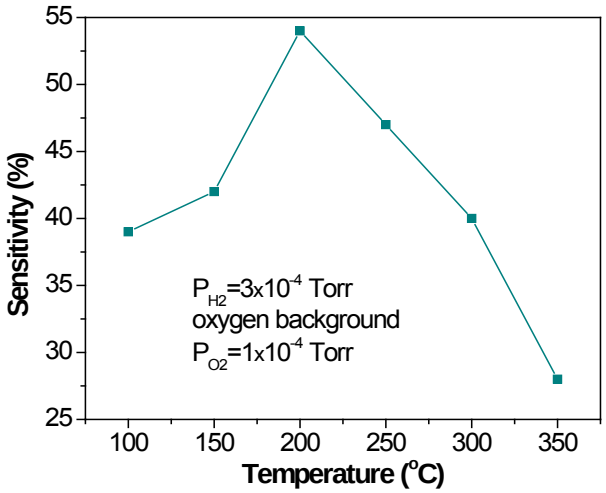

Figure 7. Temperature dependence of SMNW gas sensitivity to H_2

As in traditional thin film or ceramic based SnO_2 sensors, the interaction of hydrogen with oxygen and hydroxyl groups chemisorbed on the NW surface leads to the formation of water molecules, which at these temperatures are desorbed from NW surface. This process is

accompanied by electron release back to the conduction band of metal oxide nanowire and as result, determines the consequent NW resistance decrease drop. The observed on S=f(T) maximum is related to the competition of at least two surface processes: the thermally activated reaction with pre-adsorbed oxygen to form water molecules (electron donating path) and formation of the OH^- (electron accepting path). The first process takes place at lower temperatures while the formation of OH^- radicals is observed at higher temperatures.

Finally, to estimate the role of the namely bottlenecked segments in sensing performance of the SMNW the comparative series of measurements were carried out (in the same run) on a straight SnO_2 NW of similar length and a diameter ~100 nm. It was established that measured even at a little bit higher hydrogen pressure $P_{H2}=4x10^{-4}$ sensitivity *S* of straight nanostructure has amounted only 40%, i.e. lower than in the case of SMNW. Since the straight NW diameter is almost 3 times smaller than the average diameter (D~280 nm) of the structurally modified (containing large and narrow segments) NS, we could expect that sensitivity of the straight NW will be higher. However, we observe the opposite situation; in our opinion, it is attributed to the role played by the narrowed (~ 40-80 nm) segments in the NW conductance. In some degree, it is similar to the intergrain effects in nano/microcrystalline films or ceramic powder nanomaterials (Figure 8a). However, in our case, we have monocrystalline NS, in which larger diameter segments are alternating with narrow "necks" (Figure 8b). These narrow segments, due to their smaller diameters and, as a result, smaller diameters of the conduction channel X_2, are more sensitive to gas atmosphere changing, because at the same depth of modulation of the depletion region, the conduction channel width in the narrow segment X_2 will be smaller by a few times or even by an order than the same parameter X_1 in the large-diameter segment. At the interaction with ambient gas, this narrowed part of SMNW will be most sensitive to the presence

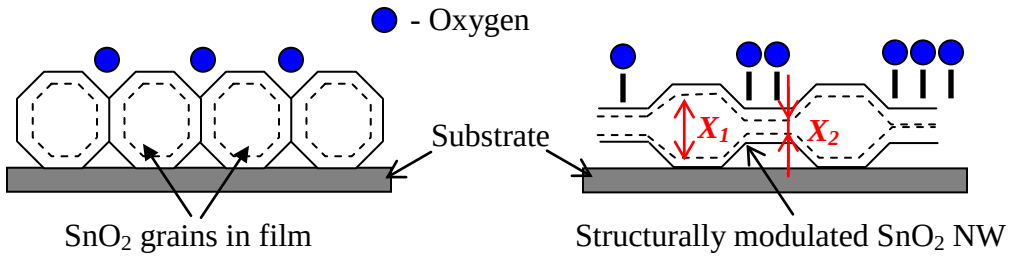

a) b)

Figure 8. Schematic presentation of interaction of the polycrystalline SnO_2 thin film (a) and single crystal SnO_2 SMNW (b) with oxygen. Dashed line shows the level of charge carrier depletion.

of different gases on its surface due to the faster depletion of the NW.

The main difference between the two cases presented in Figure 8 is that in our case the narrower segments are fabricated as integral portions of the nanowires without destroying its single-crystal morphology. The later makes it possible, in comparison with granular structures, to minimize or exclude such undesirable effects as aging, thermal, mechanical, and chemical instabilities in local intergrain interfaces.

CONCLUSIONS

In the performed research work it was shown that structurally modified single-crystal nanostructures can be successfully used in gaseous sensorics in the ppm and sub-ppm range.

The basic advantage of such monocrystalline quasi-1D nanosensors over the traditional sensors on the basis of nanostructured (nanogranular) thin film consists in the absence of the unstable intergrain contacts. Practically, nanosensor consists of the only nanowire with structurally and compositionally well-defined conducting channel. Using specially developed approach to the flow control during nanowire synthesis, it becomes possible to controllably tune the size and morphology of the single crystal NW and, as result, the size of conducting channel. In fact, we obtain an additional tool for nanostructures engineering, which renders possible to design a nanodevice for specific applications.

ACKNOWLEDGEMENTS

Author would like to thank Dr. A. Kolmakov for the possibility to carry out the research in his Laboratory of the Surface Phenomena & Imaging of Nanostructures (Southern Illinois University –Carbondale (SIUC), USA). The performed research was supported via SIUC Seed Grant and in some part through the Materials Technology Center (SIUC) Grant.

REFERENCES

1.] Y. Cui, Q.Q. Wei, H.K. Park, and C.M. Lieber, Nanowire Nanosensors for Highly Sensitive and Selective Detection of Biological and Chemical Species, Science, 293, 1289, (2001).

2. M. Law, H. Kind, B. Messer, F. Kim, and P.D. Yang, Photochemical Sensing of NO_2 with SnO_2 Nanoribbon Nanosensors at Room Temperature, Angewandte Chemie-International Edition, v. 41, Issue 13, 2405–2408 (2002).
3. E. Comini, G. Faglia, G. Sberveglieri, Z.W. Pan, and Z.L. Wang, Stable and highly sensitive gas sensors based on semiconducting oxide nanobeltsApplied Physics Letters, 81, Issue 10, 1869-1871, (2002).
4. M.S. Arnold, P. Avouris, Z.W. Pan, and Z.L. Wang, Field-Effect Transistors Based on Single Semiconducting Oxide Nanobelts, Journal of Physical Chemistry B, 107, 659, (2003).
5. C. Li, D.H. Zhang, X.L. Liu, S. Han, T. Tang, J. Han, and C.W. Zhou, In_2O_3 nanowires as chemical sensors, Applied Physics Letters, 82, Issue 10, 1613, (2003).
6. A. Kolmakov, Y.X. Zhang, G.S. Cheng, and M. Moskovits, Detection of CO and O 2 Using Tin Oxide Nanowire Sensors, Advanced Materials, 15, 997, (2003).
7. Y.L. Wang, X.C. Jiang, and Y.N. Xia, A solution-phase, precursor route to polycrystalline SnO2 nanowires that can be used for gas sensing under ambient conditions, Journal of the American Chemical Society, 125, 16176, (2003).
8. A. Kolmakov and M. Moskovits, Chemical sensing and catalysis by one-dimensional metal-oxide nanostructures, Annual Review of Materials Research, 34, 151, (2004).
9. D.H. Zhang, Z.Q. Liu, C. Li, T. Tang, X.L. Liu, S. Han, B. Lei, and C.W. Zhou, Detection of NO2down to ppb Levels Using Individual and Multiple In2O3Nanowire Devices, Nano Letters, 4, 1919, (2004).
10. Z.Y. Fan, D.W. Wang, P.C. Chang, W.Y. Tseng, and J.G. Lu, ZnO Nanowire Field Effect Transistor and Oxygen Sensing Property, Applied Physics Letters, 85, 5923, (2004).
11. B.J. Murray, E.C. Walter, and R.M. Penner, Amine Vapor Sensing with Silver Mesowires, Nano Letters, 4, 665, (2004).
12. R.E. Cavicchi, S. Semancik, F. DiMeo, and C.J. Taylor, Featured Article: Use of Microhotplates in the Controlled Growth and Characterization of Metal Oxides for Chemical Sensing, Journal of Electroceramics, 9, 155, (2003).
13. M.E. Franke, T.J. Koplin, and U. Simon, “Metal and Metal Oxide Nanoparticles in Chemiresitors: Does the Nanoscale Matter?”, Small, 2, 36, (2006).
14. G. Eranna, B.C. Joshi, D.P. Runthala, and R.P. Gupta, Oxide Materials for Development of Integrated Gas Sensors—A Comprehensive Review, Critical Reviews in Solid State and Materials Sciences, 29, 111, (2004).

15. N. Barsan, M. Schweizer-Berberich, and W. Gopel, Fundamental and practical aspects in the design of nanoscaled SnO2 gas sensors: a status report, Fresenius Journal of Analytical Chemistry, 365, 287, (1999).
16. Z.R. Dai, Z.W. Pan, and Z.L. Wang, Novel Nanostructures of Functional Oxides Synthesized by Thermal Evaporation", Advanced Functional Materials, 13, 9, (2003).
17. A. Kolmakov, D.O. Klenov, Y. Lilach, S. Stemmer, and M. Moskovits, Enhanced Gas Sensing by Individual SnO_2 Nanowires and Nanobelts Functionalized with Pd Catalyst Particles, Nano Letters, 5, 667, (2005)
18. S. Samson and C.G. Fonstad, J., Defect structure and electronic levels in stannic oxide crystals, Appl. Phys., 44, 4618, (1973).